the hot wall, comparing with a wall without fin for $Ra=10^4$. The influence of the Rayleigh number, the length and the position of the thin fin as well as the ratio of the conductivities (fin/fluid) on the heat transfer by free convection within a differentially heated cavity is examined by Bilgen [5]. It has been found that the Nusselt number increases with Rayleigh number, but decreases with conductivity ratio and fin length. Ben-Nakhi and Chamkha [6] numerically investigated the influence of the length and angle of inclination of a fin on heat transfer by free convection in a square enclosure. The fin was placed at the middle of the hot wall. It was found that the average Nusselt number is sensitive to variation in inclination angle and fin length. An experimental and numerical study on natural convection in a square cavity with two isolated baffles is carried out by Nardini et al. [7]. The cavity with plexiglas walls is heated by four discrete sources. The obtained results show that the flow and heat transfer characteristics are profoundly influenced by different fins lengths. The recent numerical study by Attouchi et al. [8] focused on the analysis of natural convection in a cavity with finned surface where one surface is kept at periodic wall temperature. Their results indicate that the best heat transfer rate is obtained for the case of enclosure with three fins at the hot side wall.

To further improve heat transfer, another innovative technique is to use nanofluids. The latter are obtained by adding nanoparticles to a base fluid in order to improve the thermal properties of the mixture. Nanofluids based on classical nanoparticles such as Al_2O_3, CuO, TiO_2, Cu, AgO, AgO are intensively studied [9-13]. One of the developments in nanofluid is carbon nanotubes (CNTs). The thermal conductivity of CNTs is very high compared to other nanoparticles and, therefore, their use can significantly improve the thermal performance of energy installations. For these reasons, studies on CNT-based nanofluids have been conducted by Ul Haq et al. [14], Tayebi et al. [15,16] and Noranuar et al. [17]. Recently, review studies on heat transfer application of carbon-based nanofluid are carried out by Borode et al. [18] and Ali et al. [19].

Sometimes undesirable factors can alter the beneficial phenomenon of natural convection. Among these undesirable factors is the presence of a magnetic field acting on electrically conductive fluids. Indeed, the Lorentz force significantly influences the heat transfer and the flow of cooling fluids. Ghasemi et al. [20] have numerically studied the natural convection of a water-Al_2O_3 nanofluid confined in an enclosure exposed to a magnetic field. Their results show that heat transfer rate increases with increasing Rayleigh number but decreases as Hartmann number increases. Sourtiji et al. [21] studied the effect of the magnetic field on the heat transfer by natural convection in L-shaped enclosures filled with nanofluid. The problem of natural convection and entropy generation of nanofluids confined in a cavity maintained at a sinusoidal temperature distribution and subjected to a magnetic field is studied numerically by Mejri et al. [22], using the lattice Boltzmann method. Belhaj and Ben-Beya [23] performed a numerical study on heat transfer by natural convection within a square cavity filled with CNT-water nanofluid and subjected to the action of a constant magnetic field. The enclosure is heated from below with a sinusoidal temperature distribution. Hamid et al. [24] studied numerically by the finite element method the hydromagnetic flow and heat transfer of water-based carbon nanotubes (CNTs) inside a rectangular fin-shaped cavity. Recently, Sarala et al. [25] have studied the effects of MHD alumina-water nanofluid flow past an oscillating vertical plate in the presence of radiation and Hall effects.

We note that the majority of research work is carried out on numerical simulation of the flow and thermal transfer of nanofluids based on classical nanoparticles such as Cu, Al_2O_3, TiO_2, etc. However, little studies has been done on nanofluids based on carbon nanotubes. In this context, the present work constitutes a contribution to the numerical study of natural hydromagnetic convection of CNT-water nanofluid confined in an enclosure heated by two isothermal fins.

PHYSICAL MODEL AND MATHEMATICAL FORMULATION

Figure 1 illustrates the configuration studied. It is a square enclosure, filled with water containing different concentrations of single walled carbon nanotubes (SWCNTs) and heated by two horizontal thin fins. The two horizontal walls and the left vertical wall are adiabatic, whereas the right wall is operated at a lower temperature (T_C). The fins are located at the left wall and maintained at high temperature (T_H). (L), (s) and (d) are representing lengths, positions and spacing of two fins, respectively. A horizontal uniform magnetic field B_o is imposed. The nanofluid is assumed to be incompressible and the density in the buoyancy force is evaluated by the Boussinesq approximation [26].This model considers density constant in all basic equations except the buoyancy term in the momentum equation. The equation below obtained using the Boussinesq approximation [26]:

$$\rho_{nf} = \rho_0[1 - \beta(T - T_0)] \tag{1}$$

Table 1 presents the thermophysical properties of water and SWCNT [27]. The viscous dissipation and joule heating are neglect.

Therefore, the conservation equations, in non dimensional form, are established below in two-dimensional [20]:

$$\frac{\partial U}{\partial X} + \frac{\partial V}{\partial Y} = 0 \tag{2}$$

$$U\frac{\partial U}{\partial X} + V\frac{\partial U}{\partial Y} = -\frac{\partial P}{\partial X} + \frac{\mu_{nf}}{\rho_{nf}\alpha_f}\left(\frac{\partial^2 U}{\partial X^2} + \frac{\partial^2 U}{\partial Y^2}\right) \tag{3}$$

$$U\frac{\partial V}{\partial X} + V\frac{\partial V}{\partial Y} = -\frac{\partial P}{\partial Y} + \frac{\mu_{nf}}{\rho_{nf}\alpha_f}\left(\frac{\partial^2 V}{\partial X^2} + \frac{\partial^2 V}{\partial Y^2}\right) + \frac{(\rho\beta)_{nf}}{\rho_{nf}\beta_f}Ra Pr\theta - Ha^2 Pr V \tag{4}$$

$$U\frac{\partial\theta}{\partial X}+V\frac{\partial\theta}{\partial Y}=\frac{\alpha_{nf}}{\alpha_f}\left(\frac{\partial^2\theta}{\partial X^2}+\frac{\partial^2\theta}{\partial Y^2}\right) \quad (5)$$

Where, the following non dimensional parameters are used:

$$X=\frac{x}{H},\quad Y=\frac{y}{H},\quad U=\frac{uH}{\alpha_f},\quad V=\frac{vH}{\alpha_f},$$
$$P=\frac{pH^2}{\rho_{nf}\alpha_f{}^2},\quad \theta=\frac{T-T_C}{T_H-T_C} \quad (6)$$
$$Ra=\frac{g\beta_f H^3(T_H-T_C)}{\upsilon_f\alpha_f},\quad Pr=\frac{\upsilon_f}{\alpha_f},\quad Ha=B_0H\sqrt{\frac{\sigma_{nf}}{\rho_{nf}\upsilon_f}}$$

The non dimensional boundary conditions are as follows:

- On the right wall: $U=V=0,\ \theta=0$ (7.a)
- On the left wall: $U=V=0,\ \frac{\partial\theta}{\partial X}=0$ (7.b)
- On the bottom wall: $U=V=0,\ \frac{\partial\theta}{\partial Y}=0$ (7.c)
- On the top wall: $U=V=0,\ \frac{\partial\theta}{\partial Y}=0$ (7.d)
- On the fins: $U=V=0,\ \theta=1$ (7.e)

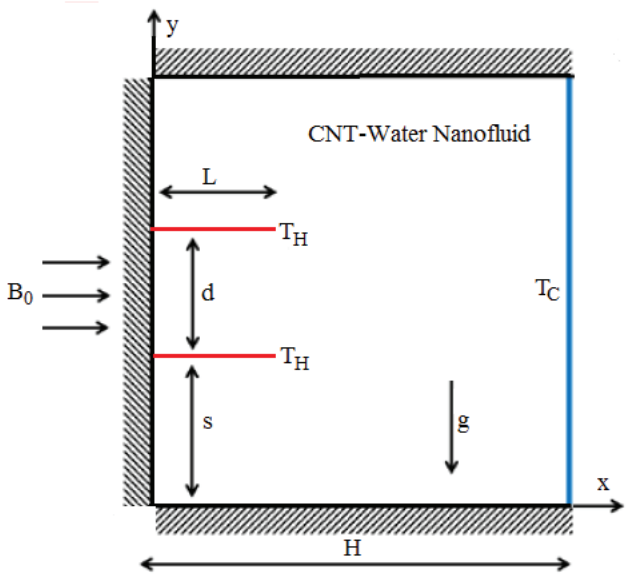

Figure 1. Physical configuration.

The properties of the nanofluid are calculated as follows [28,20]:

$$\rho_{nf}=(1-\phi)\rho_f+\phi\rho_p \quad (8)$$

$$(\rho\beta)_{nf}=(1-\phi)(\rho\beta)_f+\phi(\rho\beta)_p \quad (9)$$

$$(\rho Cp)_{nf}=(1-\phi)(\rho Cp)_f+\phi(\rho Cp)_p \quad (10)$$

$$\alpha_{nf}=\frac{k_{nf}}{(\rho Cp)_{nf}} \quad (11)$$

$$\sigma_{nf}=(1-\phi)\sigma_f+\phi\sigma_p \quad (12)$$

The dynamic viscosity and thermal conductivity of the nanofluid can beestimated by Brinkman [29] and Maxwell [30] models, respectively.

$$\mu_{nf}=\frac{\mu_f}{(1-\phi)^{2.5}},\ k_{nf}=k_f\left[\frac{(k_p+2k_f)-2\phi(k_f-k_p)}{(k_p+2k_f)+\phi(k_f-k_p)}\right], \quad (13)$$

The stream function is evaluated as following:

$$U=\frac{\partial\psi}{\partial Y}\ \text{and}\ \ V=-\frac{\partial\psi}{\partial X} \quad (14)$$

Local and average Nusselt numbers along the cold wall are evaluated as:

$$Nu_Y=-\frac{k_{nf}}{k_f}\frac{\partial\theta}{\partial X}\bigg|_{X=1} \quad (15)$$

$$Nu_m=\int_0^1 Nu_Y\,dY \quad (16)$$

NUMERICAL METHODOLOGY

The system of equations (2) - (5) associated with the boundary conditions (7.a) - (7.e) are discretized by the control volume method established by Patankar [31] employing the power law scheme. The velocity-pressure couplingis realised by the SIMPLE algorithm [31]. The tridiagonal matrix algorithm method is used to solve algebraic equations iteratively.

Table 1. Properties of water and SWCNT at 298 K [27]

	ρ (kg.m^{-3})	C_p (J.kg^{-1}.K^{-1})	k (W.m^{-1}.K^{-1})	β (K^{-1})	σ (S.m^{-1})
Pure water	997.1	4179	0.613	21×10^{-5}	0.05
SWCNT	2600	425	6600	0.16×10^{-5}	4.8×10^{7}

Table 2. Influence of mesh size on Nu_m et $|\psi|_{max}$

Grid size (X×Y)	Nu_m	Error %	$\|\psi\|_{max}$	Error %
41×41	6.9373	–	13.3122	–
61×61	6.8159	1.750	13.1135	1.492
81×81	6.7596	0.826	13.0382	0.574
101×101	6.7272	0.479	13.0083	0.229
121×121	6.7090	0.270	12.9921	0.124
141×141	6.6971	0.177	12.9843	0.060

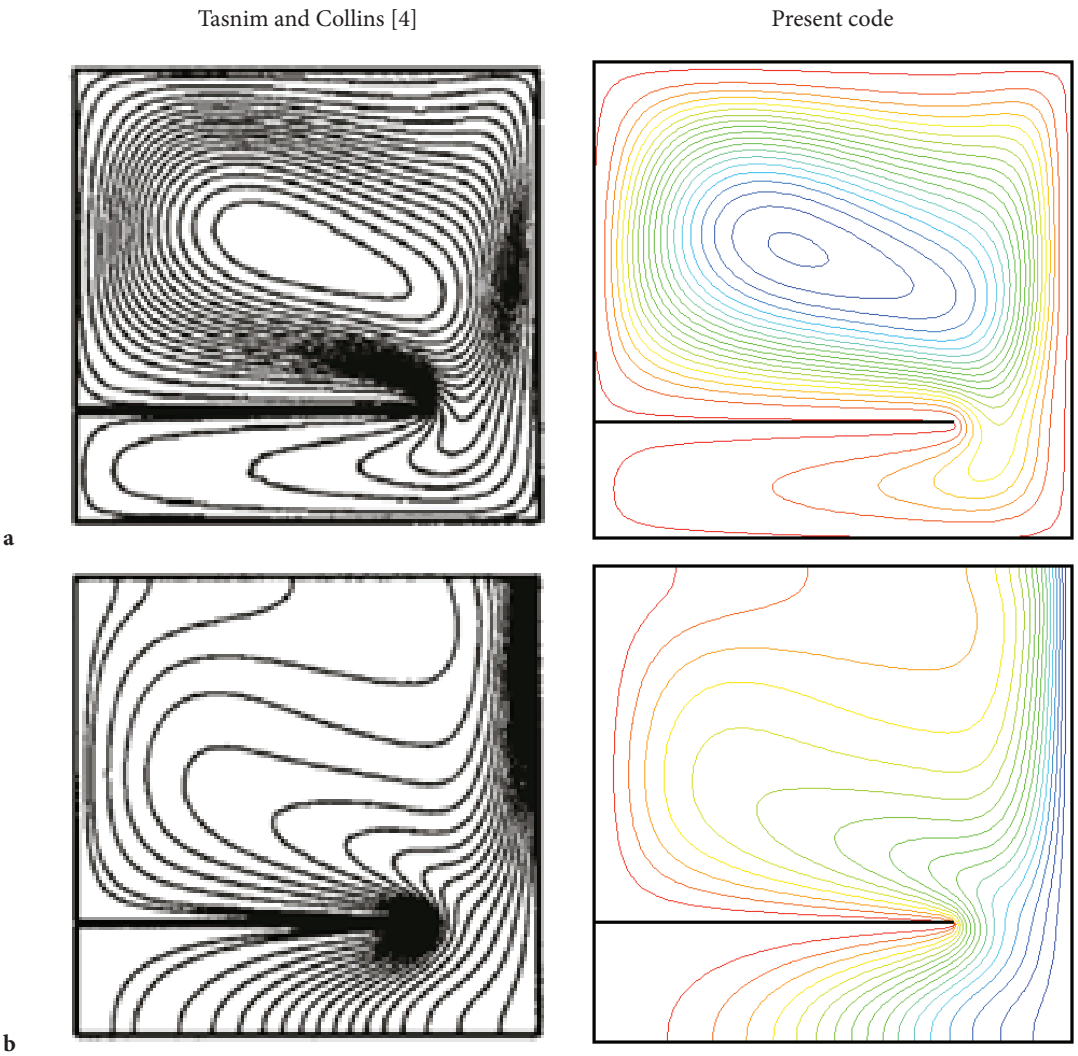

Figure 2. (a) Streamlines, (b) isotherms for $Ra=10^5$ and Pr=0.7.

Table 2 regroup the tests carried out to follow the sensitivity of the results to the mesh and this, for $Ra=10^6$, Ha=30, ϕ=0.03, L=0.25, S=0.4, D=0.2 and it appears that Nu_m and $|\psi|_{max}$ become insensitive to the number of nodes from the grid 121×121. In the continuation of our work, the 121×121 mesh is chosen to perform the simulations due to the precision/computation time compromise.

To validate the computer code developed and programmed in FORTRAN language, we compare our results with those of the literature. First, we qualitatively compared the structure of the flow and the isotherms obtained by Tasnim and Collins [4], for the case of free convection in a square enclosure with a baffle placed on the hot wall. From the Figure 2, a great similarity is observed between the

streamlines and the isotherms, obtained by our computer code and those of the reference [4].

In addition, a quantitative validation is carried out by confronting our results with those obtained by Ghasemi et al. [20] and Teamah et al. [32], who numerically treated the case of natural convection within a closed square cavity, filled with a nanofluid and exposed to a magnetic field. The comparison illustrated in Figure 3 shows the evolution of the mean Nusselt number as a function of the Hartmann number. It is clear from this figure, that there is a very satisfactory agreement between our results and those obtained by the authors.

RESULTS AND DISCUSSION

In this study, the Rayleigh number (Ra), the Hartmann number (Ha), the volume fraction of nanoparticles (ϕ), the fins position (S), the fins length (L), and the spacing of two fins (D) are considered to be within the following ranges: $10^3 \le Ra \le 10^6$, $0 \le Ha \le 60$, $0 \le \phi \le 0.06$, $0.25 \le L \le 0.75$, $0.1 \le S \le 0.7$, and $0.2 \le D \le 0.8$.

Effect of Hartmann Number (Ha) and Rayleigh Number (Ra)

The streamlines and isotherms are plotted in Figure 4a and 4b, respectively, for Rayleigh number (Ra $=10^4$, 10^5, 10^6) and Hartmann number (Ha=0, 30, 60). It is assumed that ϕ=0.03, L=0.25, S=0.4, and D=0.2. Figure 4a clearly shows the buoyancy driven circulating flows in the cavity for all Rayleigh and Hartmann numbers. As the Hartmann number increase, the strength of the circulations decreases. Indeed, the horizontal magnetic field generates a Lorentz force which acts in the vertical direction and in the opposite direction to the buoyancy force, which has result of reducing the flow intensity of the nanofluid in the enclosure. On the other hand, the circulation cell decomposes to double-eye pattern at Ha=60 for Ra=10^4 and 10^5, however this behavior disappears when the buoyancy force becomes strong at high Rayleigh number Ra=10^6. The results also show that the application of the magnetic field affects the isotherms (Figure 4b), in particular at Ra $=10^5$. As the Hartmann number increases, the isotherms straighten almost vertically. This is an indication of transformation of heat transfer mode almost to conduction. At Ra=10^6, the effect of the Lorentz force becomes less significant and the convection mode is evident. A thermal stratification is observed in the center of the cavity and below the bottom fin.

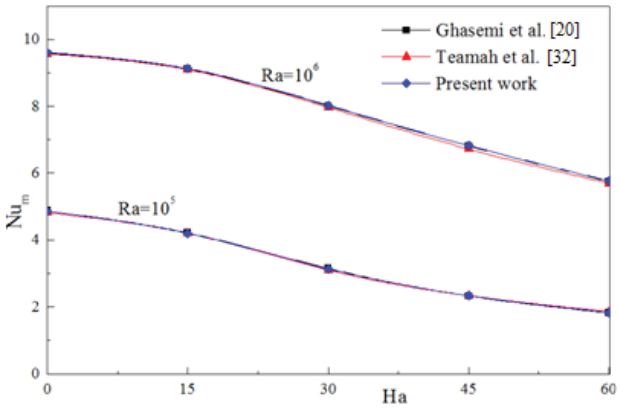

Figure 3. Comparison with the results of Ghasemi et al. [20] and Teamah et al. [32].

Figure 5 presents the influence of the Lorentz force, expressed by the variation of the Hartmann number, on the velocity (Figure 5 (a), (b) and (c)) and temperature (Figure 5 (d), (e) and (f)) profiles along the horizontal mid-span of the cavity at three Rayleigh numbers (Ra $=10^4$, 10^5 and 10^6) and for a volume fraction ϕ =0.03. It can be observed from the figure, that the maximum velocity increases under the effect of the buoyancy force, when the Rayleigh number increases and decreases when the Hartmann number increases, due to the influence of the magnetic force on the flow. The velocity profiles show that the flow between the two fins is almost stagnant for Ra=10^4 and 10^5. This is due to the convection flux which is weak. The corresponding temperature profiles show that the temperature at this location varies slowly. Increasing the Rayleigh number to 10^6 allows the nanofluid to circulate between the two fins and greatly reduces the effect of the magnetic field which manifests for the other values of the Rayleigh numbers.

The variation of the mean Nusselt number ratio ($Nu_m/Nu_{m,Ha=0}$) with the Rayleigh number at different Hartmann numbers is shown in Figure 6. It is assumed that ϕ =0.03. The $Nu_m/Nu_{m,Ha=0}$ is insensitive to the variation of the Hartmann number at Ra=10^3 because the heat transfer regime is dominated by conduction. It is clearly seen that for all Hartmann numbers, when the Rayleigh number increases up to Ra=10^4, the $Nu_m/Nu_{m,Ha=0}$ decreases because the magnetic field reduces the effect of convection flows. Moreover, we notice that for a given Rayleigh number, except Ra=10^3, the $Nu_m/Nu_{m,Ha=0}$ decreases when Hartmann number increases.

Effect of Position (S), Length (L) and Spacing (D) of Thin Fins

Figure 7 presents the streamlines (left) and the isotherms (right) for Ra=10^5 and for different fins positions (S=0.1, 0.3, 0.5, and 0.7). We observe from the figure that, when the two fins are placed very close to the bottom wall (S=0.1), the center of the recirculation cell is almost in the middle of the cavity. As the position increases, the center of the recirculation cell moves right up and the flow intensity decreases (see Table 3) due to flow clogging between the top wall and the top fin. At S=0.7, the fluid in the lower part of the cavity becomes almost motion less and colder, as shown in Figure 7.

Figures 8–10 illustrate, respectively, the effects of the fins position, the fins length and the spacing of two fins on the mean Nusselt number at different Rayleigh numbers,

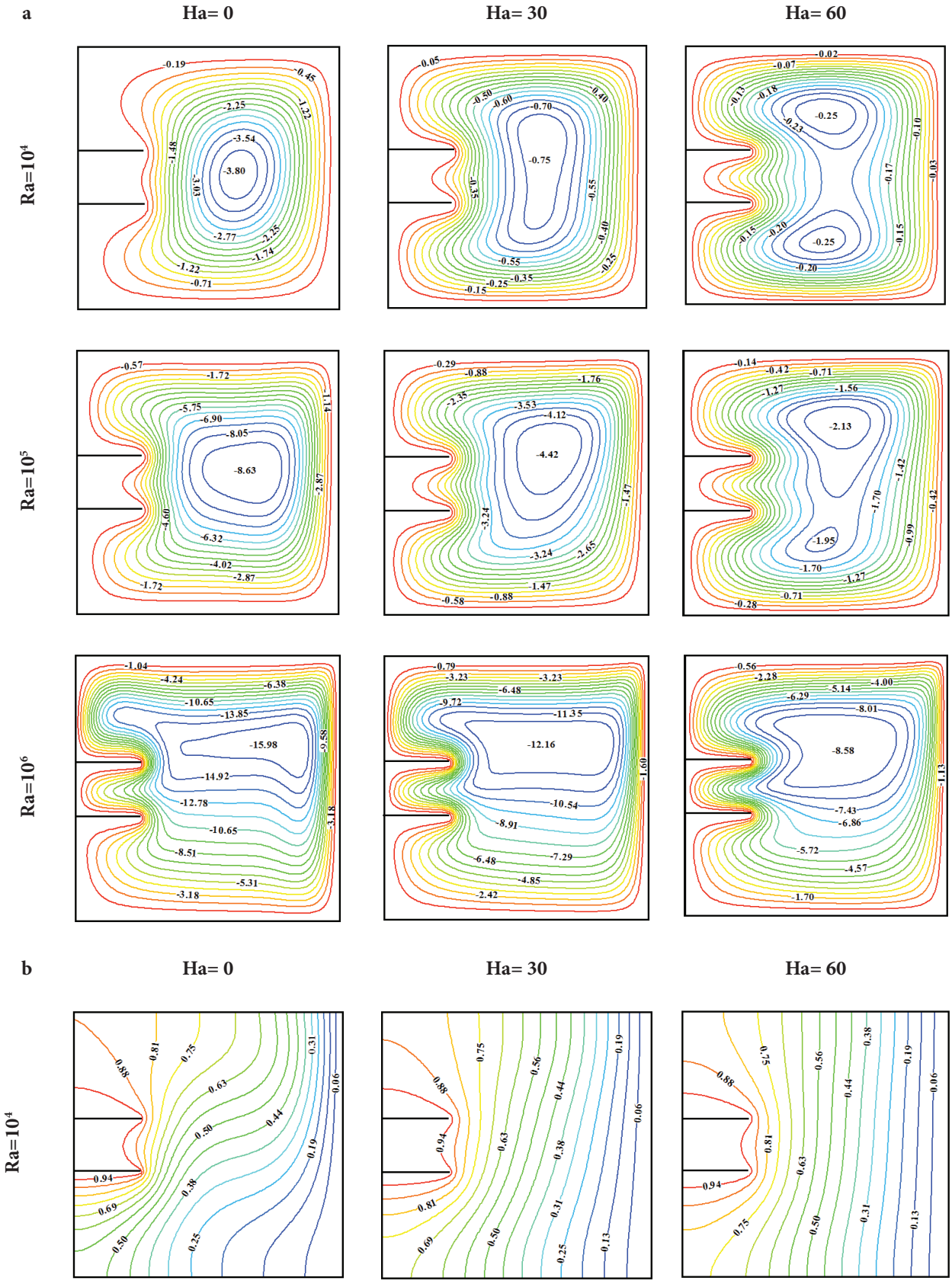

Figure 4. Continued

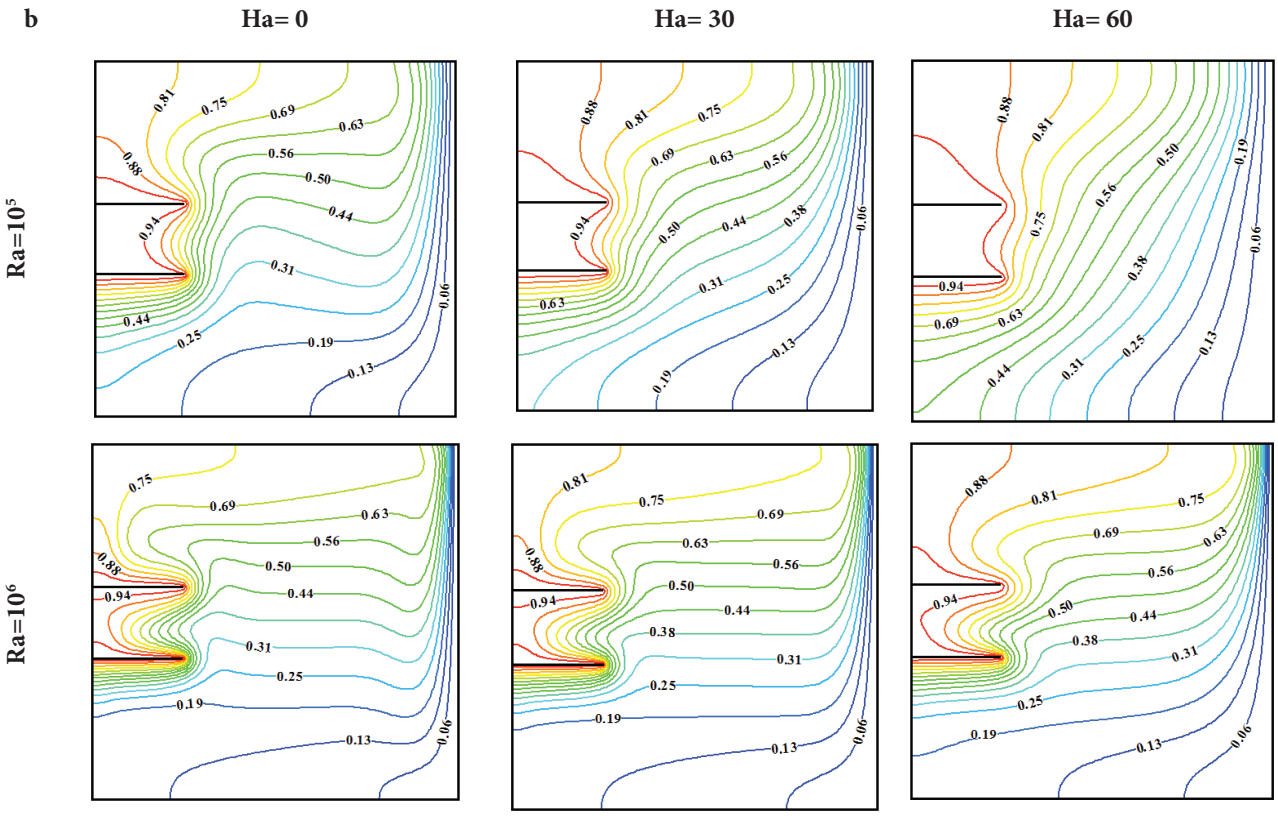

Figure 4. (a) Streamlines, (b) Isotherms for different Rayleigh and Hartmann numbers.

for ϕ=0.03 and Ha=30. It can be seen from Figure 8 that at any position S, mean Nusselt number increases as Rayleigh number increases. At low Rayleigh numbers (Ra=10^3 and 10^4), the variation in position has no significant effect on the heat transfer rate. However, at high Rayleigh numbers (Ra=10^5 and 10^6), where heat transfer is dominated by convection, the influence of position on the heat transfer rate is discernible. Indeed, the mean Nusselt number increases with increasing position until it reaches a maximum then it begins to decrease with further increase in position. As shown in Table 3 and Figure 8, the maximum mean Nusselt number occurs at S=0.3.

The influence of fins length on mean Nusselt number is presented in Figure 9. It can be observed that the heat transfer rate increases with Rayleigh number for any fins length, as the increase in the Rayleigh number improves buoyancy force and therefore augments the heat transfer rate. The mean Nusselt number is also improved with increasing fins length. This improvement can be attributed to the increase in heat transfer surface area as the length of the fins increases. The effect of fins spacing on the mean Nusselt number is shown in Figure 10. We note from the figure that the heat transfer rate increases with Rayleigh number independently of the value of fins spacing on the one hand, and that the variation of the mean Nusselt number with the fins spacing is not significant at low Rayleigh numbers, on the other hand. The maximum mean Nusselt number corresponds respectively to spacing D=0.5 and 0.3 for Ra=10^5 and 10^6.

Effect of Solid Volume Fraction (ϕ)

To examine the effect of nanoparticle concentration on heat transfer rate, the ratio between the mean Nusselt number and mean Nusselt number without volume fraction ($Nu_m/Nu_{m,\ \varphi=0}$) is illustrated in Figure 11. In the figure, for a given Ra, the Nusselt number ratio increases with increasing volume fraction. This enhancement is due to the improvement of the nanofluid thermal conductivity as the volume fraction increases. The results also show that for Ra=10^3, the volume fraction has a major effect on the heat transfer rate, however it has a minor effect at Ra=10^5. For example, when the volume fraction increases from 0 to 0.06 , the mean Nusselt number enhances about 21% at Ra=10^3 and about 1% at Ra=10^5.

Maxwell Versus Xue Models

This section presents acomparison between two models that are used to calculate the thermal conductivity of nanofluids: Maxwell model [30] and Xue model [33] which is defined as follows:

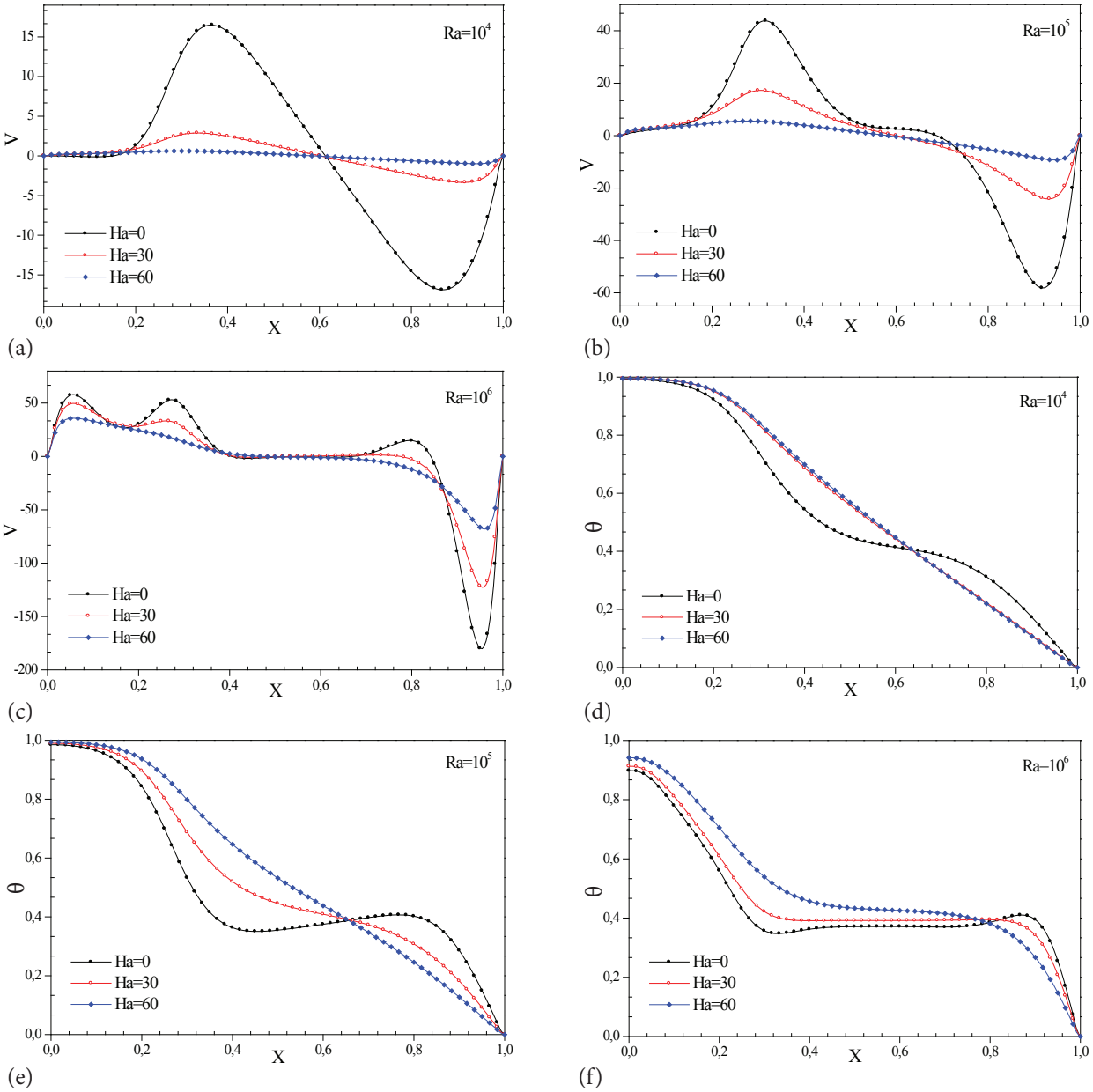

Figure 5. (a), (b) and (c) vertical velocity profile, (d), (e) and (f) temperature profile at Y = 0.5 for ϕ = 0.03, L = 0.25, S = 0.4 and D = 0.2.

$$k_{nf} = k_f \left[\frac{1 - \phi + 2\phi \frac{k_p}{k_p - k_f} ln \frac{k_p + k_f}{2k_f}}{1 - \phi + 2\phi \frac{k_f}{k_p - k_f} ln \frac{k_p + k_f}{2k_f}} \right] \quad (17)$$

In fact, the models used to evaluate the properties of nanofluids and in particular those relating to thermal conductivity, considerably affect the thermal performance of nanofluids [34, 35]. The theoretical model proposed by Xue is based on Maxwell theory and takes into consideration the rotating elliptical nanotubes with a important axial ratio [17]. The results obtained so far are based on the Maxwell model [30].

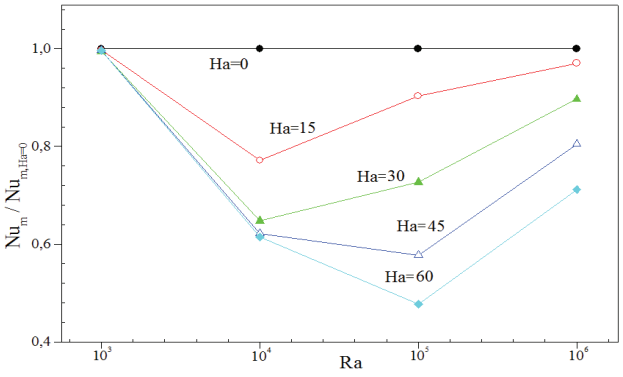

Figure 6. Evolution of mean Nusselt number ratio with Ra for L=0.25, S=0.4 and D=0.2.

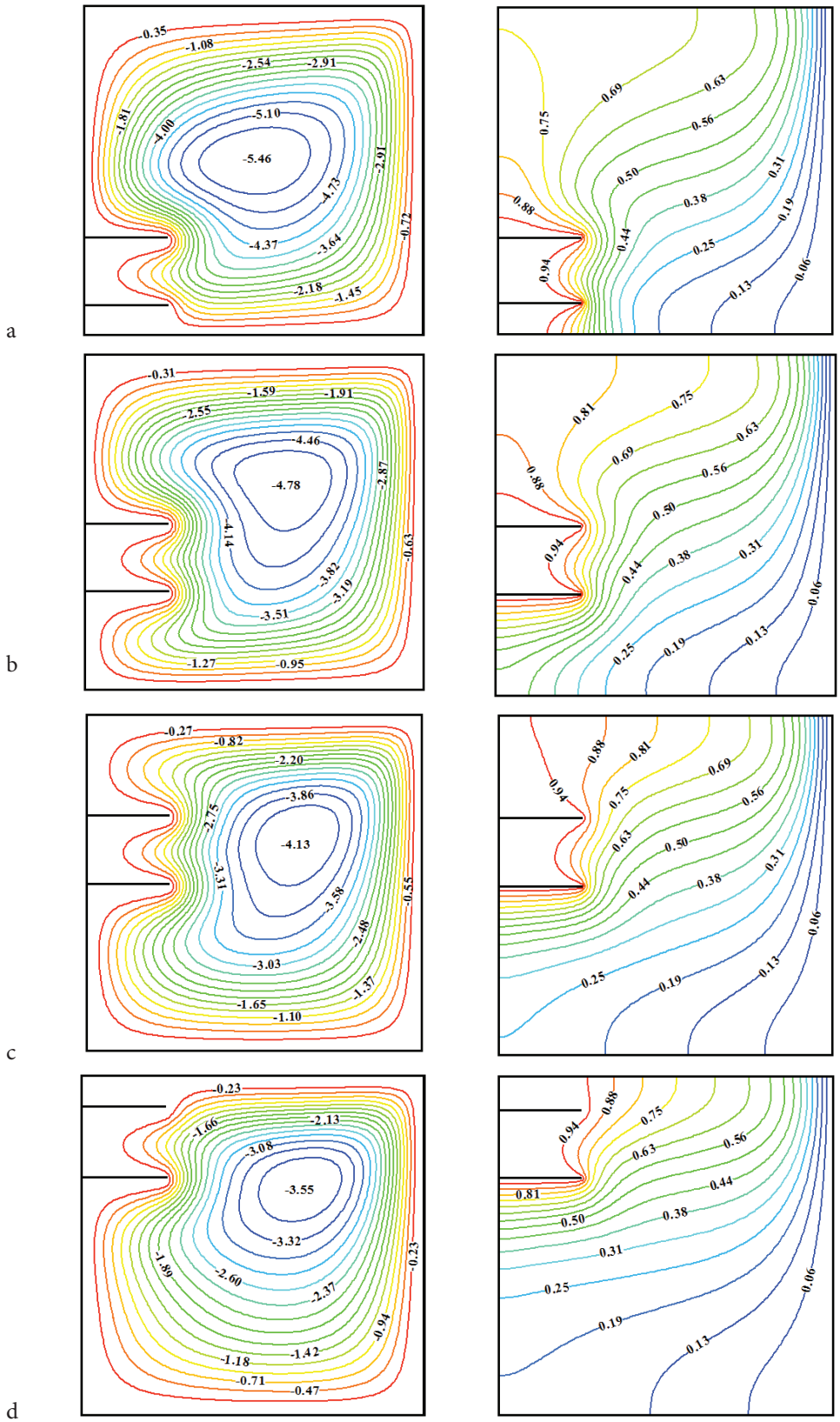

Figure 7. Streamlines (left) and isotherms (right) for Ra=10^5, Ha=30, L=0.25, D=0.2 and ϕ=0.03, (a) S=0.1, (b) S=0.3, (c) S=0.5, (d) S=0.7.

Table 3. Nu_m and $|\psi|_{max}$ at various Ra and S (L=0.25, D=0.2, ϕ =0.03 and Ha=30)

		S=0.1	S=0.3	S=0.5	S=0.7
$Ra=10^3$	Nu_m	1.0904	1.2021	1.1753	1.0420
	$\|\psi\|_{max}$	0.0915	0.0877	0.0857	0.0873
$Ra=10^4$	Nu_m	1.1772	1.2763	1.2527	1.1138
	$\|\psi\|_{max}$	0.9609	0.8772	0.7914	0.7758
$Ra=10^5$	Nu_m	2.6945	2.8288	2.5418	2.0462
	$\|\psi\|_{max}$	5.8383	5.1110	4.4148	3.7932
$Ra=10^6$	Nu_m	6.8154	7.0009	6.2250	4.6662
	$\|\psi\|_{max}$	17.8165	14.7509	11.6565	9.2761

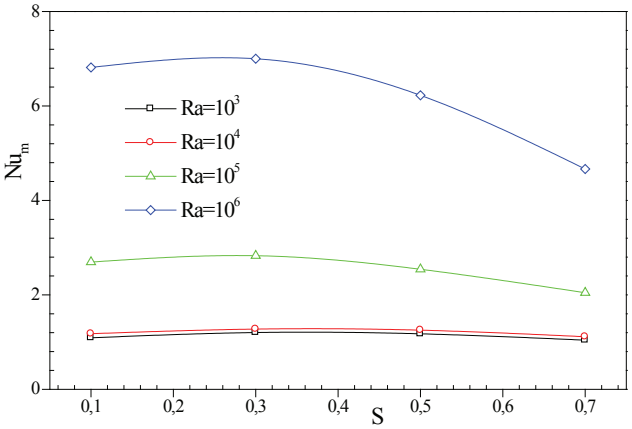

Figure 8. Evolution of Nu_m with S at different Ra for L=0.25, D=0.2and Ha=30.

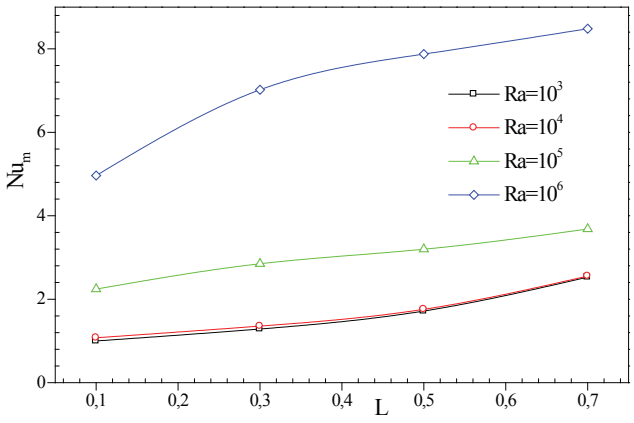

Figure 9. Evolution of Nu_m with L at different Ra for S=0.4, D=0.2 and Ha=30.

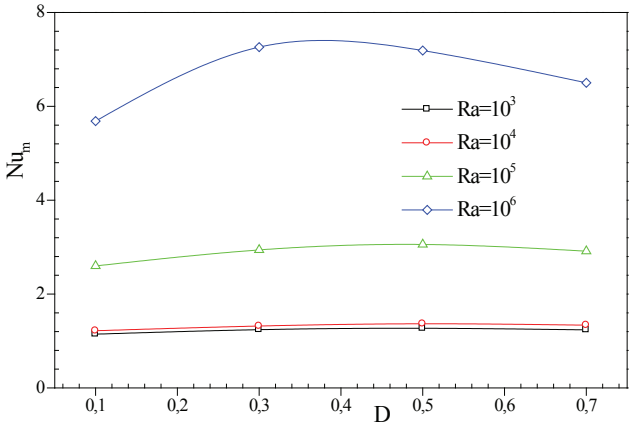

Figure 10. Evolution of Nu_m with D at different Ra for L=0.25 and Ha=30.

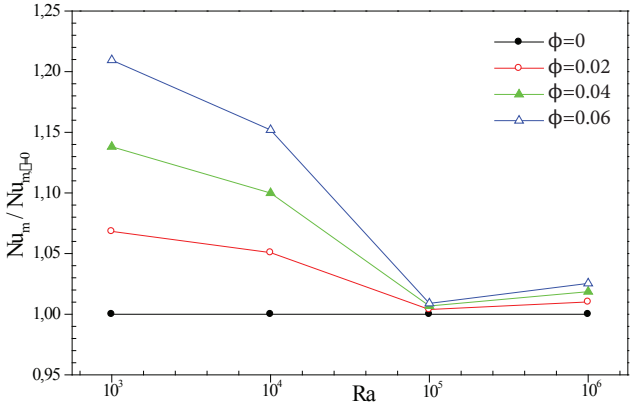

Figure 11. Evolution of mean Nusselt number ratio with Ra for Ha=30, L=0.25, S=0.4 and D=0.2

Figure 12 examines the variation in the mean Nusselt number ratio ($Nu_m/Nu_{m,\,\varphi=0}$) with the volume fraction at different Rayleigh numbers, for the two models. The results, which are presented for Ha=30, L=0.25, S=0.4, and D=0.2 show that the mean Nusselt number ratio obtained with Xue's model is higher than that obtained using Maxwell's model. Furthermore, the results reveal that for all Rayleigh numbers and for both models, when the volume fraction increases the mean Nusselt number ratio increases. This increase is

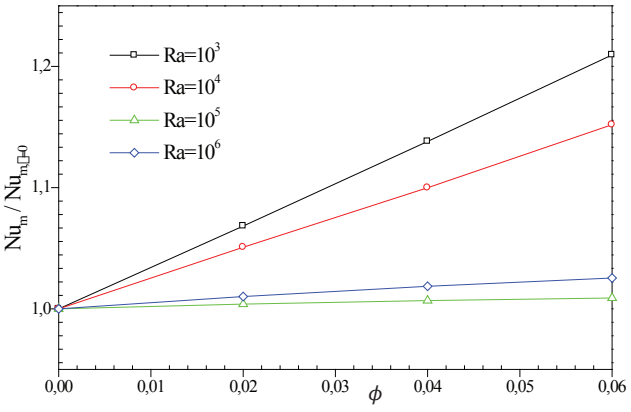

(a)

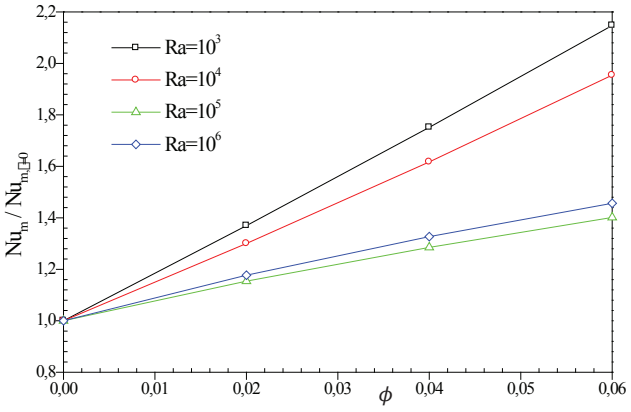

(b)

Figure 12. Evolution of mean Nusselt number ratio with ϕ for Ha=30, L=0.25, S=0.4, and D=0.2, (a) Maxwell model, (b) Xue model.

accentuated at low Rayleigh numbers because the introduction of nanoparticles improves the thermal conductivity of nanofluid which increases the mode of heat transfer by conduction. The results relating to the Xue model for ϕ=0.06 indicates that the mean Nusselt number ratio is about 2.14, 1.95, 1.40 and 1.45 for Ra =10^3, 10^4, 10^5 and 10^6, respectively. However, the results obtained with Maxwell's model indicate that the mean Nusselt number ratio is about 1.20, 1.15, 1.01 and 1.02 for Ra=10^3, 10^4, 10^5 and 10^6, respectively.

CONCLUSION

In this study, MHD natural convection heat transfer of carbon nanotube-water nanofluid in square enclosure under a magnetic field and including two isothermal thin fins is numerically investigated. The effects of Hartmann number, Rayleigh number, positon of the fins, length of the fins, spacing of the two fins and volume fraction of nanoparticles are analysed. The results obtained revealed the following points:

- Application of the magnetic field results in significant changes in the flow structure, especially if the Hartmann number is high and the Rayleigh numbers are low.
- The flow strength increases with the increase in the Rayleigh number and decreases when the Hartmann number increases.
- The application of the magnetic field also modifies the temperature distribution in the cavity, in particular at Ra =10^5, however the effect of the magnetic force becomes less significant At Ra=10^6.
- When the Rayleigh number is between 10^4 and 10^5, the heat transfer rate increases or decreases depending on the value of the Hartmann number. But, beyond Ra=10^5, there is an improvement in heat transfer for any value of the Hartmann number.
- At low Rayleigh numbers (Ra=10^3 and 10^4), the average Nusselt number is not sensitive either to the variation in position or to the spacing of the two fins.
- The increase in fins length leads to increase in mean Nusselt number for any Rayleigh number, Whereas the optimal heat transfer rate is obtained at the position S=0.3 for all Rayleigh numbers.
- The heat transfer rate improves with increasing concentration of nanoparticles, the effect of which is important at low Rayleigh number.
- The heat transfer rates obtained using the Maxwell model are lower than those obtained using the Xue model.

As future extension to this work, the heterogeneous dynamic model due to the heterogeneity of the nanofluid induced by thermophoresis diffusions and brownian motion, may be investigated.

NOMENCLATURE

B_0	Strength of the magnetic field, T
Cp	Specific heat, $J.kg^{-1}.K^{-1}$
d	Dimensional spacing of two fins, m
D	Non dimensional spacing of two fins
g	Acceleration of gravity, $m.s^{-2}$
H	Cavity height, m
Ha	Hartmann number
k	Thermal conductivity, $W.m^{-1}.K^{-1}$
l	Dimensional thin fins length, m
L	Non dimensional thin fins length
Nu	Nussel number
p	Pressure, Pa
P	Non dimensional pressure
Pr	Prandtl number
Ra	Rayleigh number
s	Dimensional thin fins position, m
S	Non dimensional thin fins position
T	Temperature, K
u, v	velocity components, $m.s^{-1}$
U, V	Non dimensional velocities
x, y	Cartesian coordinates, m
X, Y	Non dimensional cartesian coordinates

Greeksymbols

α	Thermal diffusivity, $m^2.s^{-1}$
β	Thermal expansion coefficient, K^{-1}
θ	Non dimensional temperature
μ	Dynamic viscosity, Pa.s
υ	Kinematic viscosity, $m^2.s^{-1}$
ρ	Density, $kg.m^{-3}$
σ	Electrical conductivity, $S.m^{-1}$
ϕ	Nanoparticle volume fraction
ψ	Non dimensional stream function

Subscripts

C	Cold
f	Fluid (pure water)
H	Hot
m	Mean
max	Maximum
nf	Nanofluid
o	Reference value
p	Nanoparticle

Abbreviations

CNT	Carbon nanotube
MHD	Magnetohydrodynamic
SWCNT	Single walled carbon nanotube

AUTHORSHIP CONTRIBUTIONS

Authors equally contributed to this work.

DATA AVAILABILITY STATEMENT

The authors confirm that the data that supports the findings of this study are available within the article. Raw data that support the finding of this study are available from the corresponding author, upon reasonable request.

CONFLICT OF INTEREST

The author declared no potential conflicts of interest with respect to the research, authorship, and/or publication of this article.

ETHICS

There are no ethical issues with the publication of this manuscript.

REFERENCES

[1] De Vahl Davis G. Natural convection of air in a square cavity: A bench mark numerical solution. Int J Numer Methods Fluids 1983;3:249–264. [CrossRef]

[2] Yildiz S. Investigation of natural convection heat transfer at constant heat flux along with a vertical and inclined plate. J Therm Eng 2018;4:2432–2444. [CrossRef]

[3] Shi X, Khodadadi JM. Laminar natural convection heat transfer in a differentially heated square cavity due to a thin fin on the hot wall. J Heat Transf 2003;125:624–634. [CrossRef]

[4] Tasnim SH, Collins MR. Numerical analysis of heat transfer in a square cavity with a baffle on the hot wall. Int Commun Heat Mass Transf 2004;31:639–650. [CrossRef]

[5] Bilgen E. Natural convection in cavities with a thin fin on the hot wall. Int J Heat Mass Transf 2005;48:3493–3505. [CrossRef]

[6] Ben-Nakhi A, Chamkha AJ. Effect of length and inclination of a thin fin on natural convection in a square enclosure. Numer Heat Transf A Appl 2006;50:381–399. [CrossRef]

[7] Nardini G, Paroncini M, Vitali R. Natural convection in a square cavity with two baffles on the vertical walls: Experimental and numerical investigation. Int J Mech 2015;9:120–127.

[8] Attouchi MT, Larbi S, Khelladi S. Effect of some parameters on natural convection heat transfer in finned enclosures - A case study. Int J Thermofluid Sci Technol 2022;9:090102. [CrossRef]

[9] Santra AK, Sen S, Chakraborty N. Study of heat transfer augmentation in a differentially heated square cavity using copper water nanofluid. Int J Therm Sci 2007;47:1113–1122. [CrossRef]

[10] Ho CJ, Chen MW, Li ZW. Numerical simulation of natural convection of nanofluid in a square enclosure: Effects due to uncertainties of viscosity and thermal conductivity. Int J Heat Mass Transf 2008;51:4506–4516. [CrossRef]

[11] Aminossadati SM, Ghasemi B. Natural convection cooling of a localized heat source at the bottom of a nanofluid-filled enclosure. Eur J Mech B Fluids 2009;28:630–640. [CrossRef]

[12] Suneetha S, Subbarayudu K, Bala Anki Reddy P. Hybrid nanofluids development and benefits: A comprehensive review. J Therm Eng 2022;8:445–455. [CrossRef]

[13] El Hattab M, Lafdaili Z. Turbulent natural convection heat transfer in a square cavity with nanofluids in presence of inclined magnetic field. Therm Sci 2022;26:3201–3213. [CrossRef]

[14] Ul Haq R, Nadeem S, Khan ZH, Noor NFM. Convective heat transfer in MHD slip flow over a stretching surface in the presence of carbon nanotubes. Phys B Condens Matter 2015;457:40–47. [CrossRef]

[15] Tayebi T, Ferhat CE, Rezig N, Djezzar M. Free convection in a carbon nanotube-water nanofluid filled enclosure with power-law variation wall temperature. J Nanofluids 2016;5:531–542. [CrossRef]

[16] Tayebi T, Chamkha AJ, Djezzar M. Natural convection of CNT-water nanofluid in an annular space between confocal elliptic cylinders with constant heat flux on inner wall. Sci Iran 2019;26:2770–2783.

[17] Noranuar WNN, Mohamad AQ, Shafie S, Khan I. Unsteady free convection flow of water-based carbon nanotubes due to non-coaxial rotations of moving disk. J Appl Sci Eng 2022;25:501–510.
[18] Borode AO, Ahmed NA, Olubambi PA. A review of heat transfer application of carbon-based nanofluid in heat exchangers. Nano Struct Nano Objects 2019;20:100394. [CrossRef]
[19] Ali N, Bahman AM, Aljuwayhel NF, Ebrahim SA, Mukherjee S, Alsayegh A. Carbon-based nanofluids and their advances towards heat transfer applications-a review. Nanomaterials (Basel) 2021;11:1628. [CrossRef]
[20] Ghasemi B, Aminossadati SM, Raisi A. Magnetic field effect on natural convection in a nanofluid-filled square enclosure. Int J Therm Sci 2011;50:1748–1756. [CrossRef]
[21] Sourtiji E, Hosseinizadeh SF. Heat transfer augmentation of magnetohydrodynamics natural-convection in L-shaped cavities utilizing nanofluids. Therm Sci 2012;16:489–501. [CrossRef]
[22] Mejri I, Mahmoudi A, Abbassi MA, Omri A. Magnetic field effect on entropy generation in a nanofluid-filled enclosure with sinusoidal heating on both side walls. Powder Technol 2014;266:340–353. [CrossRef]
[23] Belhaj S, Ben-Beya B. Numerical simulation of unsteady MHD natural convection of CNT-water nanofluid in square cavity heated sinusoidally from below. Particul Sci Technol 2019;37:851–870. [CrossRef]
[24] Hamid M, Khan ZH, Khan WA, Ul Haq RU. Natural convection of water-based carbon nanotubes in a partially heated rectangular fin-shaped cavity with an inner cylindrical obstacle. Phys Fluids 2019;31:103607. [CrossRef]
[25] Sarala S, Geetha E, Nirmala M. Numerical investigation of heat transfer & hall effects on mhd nanofluid flow past over an oscillating plate with radiation. J Therm Eng 2022;8:757–771. [CrossRef]
[26] Gray DD, Giorgini A. The validity of the boussinesq approximation for liquids and gases. Int J Heat Mass Transf 1976;19:545–551. [CrossRef]
[27] Job VM, Gunakala SR, Rushi Kumar B, Sivaraj R. Time-dependent hydromagnetic free convection nanofluid flows within a wavy trapezoidal enclosure. Appl Therm Eng 2017;115:363–377. [CrossRef]
[28] Xuan Y, Roetzel W. Conceptions for heat transfer correlation of nanofluids. Int J Heat Mass Transf 2000;43:3701–3707. [CrossRef]
[29] Brinkman HC. The viscosity of concentrated suspensions and solution. J Chem Phys 1952;20:571–581. [CrossRef]
[30] Maxwell JC. A Treatise on Electricity and Magnetism. Oxford: Clarendon Press; 1891.
[31] Patankar SV. Numerical Heat Transfer and Fluid-Flow. New York, USA: Hemisphere Publishing; 1980.
[32] Teamah MA, El-Maghlany WM. Augmentation of natural convective heat transfer in square cavity by utilizing nanofluids in the presence of magnetic field and uniform heat generation/absorption. Int J Therm Sci 2012;58:130–142. [CrossRef]
[33] Xue QZ. Model for thermal conductivity of carbon nanotube-based composites. Physica B Condens Matter 2005;368:302–307. [CrossRef]
[34] Lee S, Choi SUS, Li S, Eastman JA. Measuring thermal conductivity of fluids containing oxide nanoparticles. J Heat Transf 1999;121:280–289. [CrossRef]
[35] Abu-Nada E. Effects of variable viscosity and thermal conductivity of Al2O3-water nanofluid on heat transfer enhancement in natural convection. Int J Heat Fluid Flow 2009;30:679–690. [CrossRef]